

Investigations of microstructural and mechanical properties evolution of AA1050 alloy sheets deformed by cold-rolling process and heat treatment annealing

M. Mhedhbi^{1,2*}, M. Khlif¹, C. Bradai¹

1. Electromechanical Systems Laboratory (LASEM), National School of Engineers of Sfax, University of Sfax (ENIS) PB 1173-3038, Sfax, Tunisia

2. Faculty of Sciences of Sfax (FSS), University of Sfax, B.P 802-3038, Tunisia

Received 13 Dec 2016,
Revised 22 Feb 2017,
Accepted 27 Feb 2017

Keywords

- ✓ AA1050 alloy;
- ✓ cold-rolling;
- ✓ microstructure;
- ✓ mechanical properties;
- ✓ annealing;
- ✓ Plasticity;

M.Mhedhbi
moufidamhedhbi@yahoo.com
+216 97018361

Abstract

The aim of this contribution is to study the performance of the homogenized AA1050 alloy, as well as after the different metallurgical conditions such as, cold-rolling and cold-rolling annealed. For this reason, microstructures, microhardness and tensile tests were studied. From the most important results, the optical micrographs show that with increasing cold-rolling reduction rate, the equiaxed grains are elongated along the rolling direction obviously. The accumulation of rolling reduction increases the work hardening effect, which is a good agreement with the improvement of strength and low plasticity. we can giving some values; when cold-rolling reduction is about 66 %, the ultimate tensile strength reaches 140 MPa, the microhardness is 53 HV0.3 but elongation is only 1.75 %. After cold-rolling and the annealing treatment, the SEM micrographs and the DRX patterns show more secondary phase precipitates and more intermetallic formed. With an increase of annealing temperature, the amount of precipitates increases and work hardening decrease, continuously. The elongation is improved to 36 % but the tensile strength is decreased to 86 MPa after the annealing at 350 °C for 1 hour.

1. Introduction

Aluminum alloys have attracted much more attention due to the fact that they possess light mass, high strength, good formability, high heat conductivity, high rigidity, easy recycling, excellent corrosion resistance, and important tensile strength [1-3]. For the reasons of such attractive features, they have been showing a remarkable increase in the automotive industry applications and other engineering areas, including aerospace industry and telecommunication [4-11]. Furthermore, aluminum alloys offer one of the best choices of metals for aircraft structural components due to their high performance characteristics, manufacturing costs, implementation methods and manufacturing facilities, allowing their use in large amounts in the future technology [12]. Nevertheless, it is indispensable to improve the mechanical behavior of these manufacturing materials such as strength and ductility [13]. Consequently, the most important advantage of the aluminum alloys with small thickness is not only to economize the cost, but also to reduce the weight for structural applications. Then it's a challenge to produce an alloy with enhanced resistance and keeping a reasonable ductility. For not-heat-treated aluminum alloys, resistance can be obtained by forming heavy cold, which is related to the substructure refinement resulted in large plastic deformation. However, a poor ductility is frequently accompanied by a heavy cold work such as the cold rolling. Often the annealing at a lower temperature in the beginning of recrystallization may be applied to recover ductility without significant loss of strength. [14-18]. The cold-rolling is a very important process of wide aluminum alloy sheets. Additionally, the rolling reduction and the following annealing temperature are the important parameters during this process. Certainly, the annealing heat treatment can improve the forming ability for the rolled sheet. For these reasons, in the one hand, it is important to study the effect of the cold-rolling reduction and in the second hand

the annealing temperature effect on the microstructure and on the mechanical properties of aluminum alloy [19–22].

In this perspective, the AA1050 alloy is generally characterized by low mechanical strength compared to other aluminum series, due to less solute atoms and particles which have precipitated a barrier against the mobility of dislocations. Nevertheless, this material strength could be significantly improved by severe plastic deformation [23–25]. This sheet metal is one of the most popular categories of aluminum for general sheet metal work where moderate strength is required. AA1050 alloy is used industrially as a chemical process plant equipment, food containers, lamp reflectors, architectural flashings, and cable sheathing. This could be due to its powerful corrosion resistance and high ductility properties.

The purpose of the present study is to investigate the microstructural and mechanical properties of AA1050 alloy at different metallurgical conditions. A particular interest was given to the effect of the corresponding modifications to the variation of mechanical properties as well as those of the microstructure. Our study provides a strong support to improve mechanical properties and performance of aluminum alloy sheets and thus to develop a new technology for industrial applications.

2. Experimental procedure

The material used through this investigation is AA1050 alloy, 3 mm thick sheet. The chemical composition is given in Table 1. The as-received AA1050 alloy was homogenized at 500 °C for 24 hours and finally quenched in iced water, in order to obtain a fully recrystallized homogeneous microstructure. The homogenized samples were machined into 300 mm × 300 mm × 3 mm rectangular as the as-rolled specimens. Then, sheet was rolled in air. The thickness of sheet was reduced by rolling from 3 to 1.5 mm and 1 mm, and total rolling reductions are 50 % and 66 %, respectively. The as-rolled alloy with the reduction of 66 % has been retained to study the impact of annealing temperature on microstructure of as-rolled aluminum alloys. Four types of heat treatments were performed on the as-rolled alloy, namely at 100, 200, 300 and 350 °C for 1 hour, respectively. The metallographic analysis was conducted by exposing the specimens to grinding at up from 600 to 4000 abrasive papers, fine polishing to mirror finish with diamond paste respectively of 9 μm, 6 μm, 3 μm and 1 μm and then the specimen surfaces were etched by an electrolytic etching Keller's solution reagent (2 % HF + 3 % HCl + 5 % HNO₃ + 90 % H₂O). The microstructure evolution of the samples was studied using optical microscopy (OM) and scanning electron microscopy (SEM) by an accelerating voltage of 15 kV. The phase identification was examined by a Siemens D5000 X-ray diffractometer using CuKα X ray source and 2θ range from 5° to 120° at a scanning rate of 0.02(°)/s. The XRD patterns were achieved from the sheet of the 15 mm × 10 mm × 1 mm samples, cut along longitudinal direction. Specimens for hardness tests were prepared by mechanical grinding and polishing, then conducted on a Vickers hardness testing machine with a load of 300 g and a loading duration of 15 s. For each specimen, at least ten indents were performed. Tensile tests were carried out to evaluate the mechanical properties of the AA1050 alloy. It was performed on testing machine at a cross-bar speed of 5mm / min following the standard I.S.O 6892. We make many tests to see if we obtain a good reproducibility. The extensometer attached to the sample gauge was used to determine strain and total elongation. The 0.2 % yield strength (Y.S), ultimate tensile strength (U.T.S) and elongation to failure were averaged over three specimens.

Table 1. Chemical composition in weight % of the AA1050 alloy sheet studied.

Al	Fe	Si	Mg	Mn	Ni	Cu	Cr	Zn	Pb
balanced	0.21	0.0693	≤0.05	0.0170	≤0.1	0.0823	≤0.03	≤0.15	≤0.03

3. Results and discussion

3.1 Microstructure characterization

The optical microstructures of a received state (a), homogenized (b) and as cold-rolled AA 1050 alloy with different reductions (c-d) are shown in (Figure. 1.) .The as- received alloy had a heterogeneous microstructure with grains dispersed in various directions (Figure.1a). After homogenization treatment at 500°C for 24 hours, most residual phases are dissolved into α-Al matrix, and the grain boundaries become thinner and clear (Figure. 1b). The grain shape was equiaxed. However, small indissoluble phases containing Fe and Si elements can still be observed both within the grains and along the grain boundaries.

Figure. 1c shows the OM micrograph of the AA1050 alloy after application of 50 % rolling reduction. The grains of the sample were significantly elongated with respect to the rolling direction. The shear bands were

observed at 45° angles with respect to the rolling direction. By comparison, when the strain was further increased to 66 % rolling reduction, the grains are severely elongated along the rolling direction and fibrous grains were obtained in the sample (Figure. 1d).

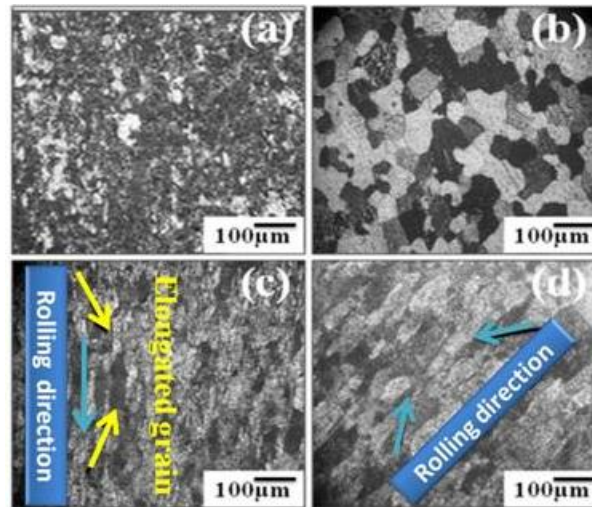


Figure. 1: Optical micrographs of a received state AA1050 alloy (a), AA1050 alloy homogenized (b), AA1050 alloy cold-rolled 50 % (c) and AA1050 alloy cold-rolled 66 % (d).

Figure 2. Illustrates the microstructures of as-rolled AA1050 alloy with 66 % reduction under different heat treatments. It can be seen that annealing treatments change the grain morphology, the grain size of the alloy is larger with the increase of annealing temperature, especially in Figure. 2(a-b). The grains grow seriously after annealing at 300 °C for 1 hour (Figure. 2c). Many intermetallic particles precipitate from the matrix during annealing and most of these precipitates are distributed along with grain boundaries after annealing treatment. It is found that the precipitates of the alloy are the most when annealing at 350°C for 1 hour (Figure. 2d). The same result confirmed by Jun-Hyun, Han et al [26].

In order to observe the change of secondary phase, further SEM and XRD studies were conducted on the all samples and the results are shown in Figs. 3, 4 and 5, respectively.

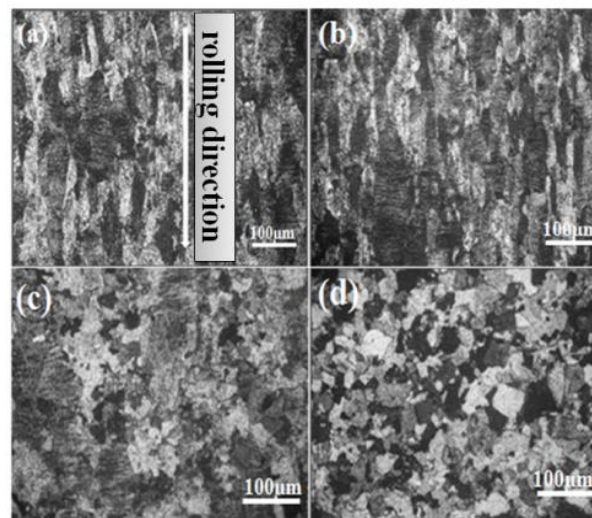


Figure. 2: Optical micrographs of as-rolled AA1050 alloy with 66% rolling reduction subjected to different annealing heat treatments: (a) cold-rolled + annealing 100°C for 1 hour, (b) 200 °C for 1 hour, (c) 300 °C for 1 hour and (d) 350 °C for 1 hour.

Figures. (3-4) show the morphology of the AA1050 alloy analyzed by SEM. The treatment of AA1050 material at the temperature of 500 ° C. for 24 hours gives it a good homogenization as shown in Figure.3c-d. Firstly the AA1050 alloy in its present state of reception (Figure.3a-b) demonstrated non-homogeneous microstructural behaviour. It shows the existence of some precipitates. This explains that values of yield strength, tensile stress and microhardness were accompanied by a low elongation [27, 28]. After cold-rolling, the SEM micrographs of

AA1050 alloy (Figure.4a-b) and (Figure.4c-d) show that the precipitates are very fine [29]. The particle morphology and the particle size distribution become nearly homogeneous. In fact the deformation by cold-rolling generating the fragmentation of the microstructure has not been canceled even by annealing at 350°C for 1 hour.

Fig.5. shows the sample at as- received presents a final texture on the plane (220). After homogenization, a new privilege texture is generated following a new plan (200). Further, It is noticed the presence of all peaks on the face-centered cubic structure of the aluminum. In addition the fundamental reflexions of the aluminum matrix are very fine XRD reflexions with low intensity are observed (figure.5a-b-c-d).These XRD reflexions correspond to the presence of a second phase and an intermetallic compound. Then, it's could be attributed to the precipitates Al_3Fe_2Si and Al_3Fe . The crystallographic structure of Al_3Fe_2Si can be judged as hexagonal structure and Al_3Fe as a monoclinic structure. Our results are in good agreement with other work done on the same alloy [29]. Even after cold-rolling and annealing at 350°C for 1 hour no changes in texture was observed.

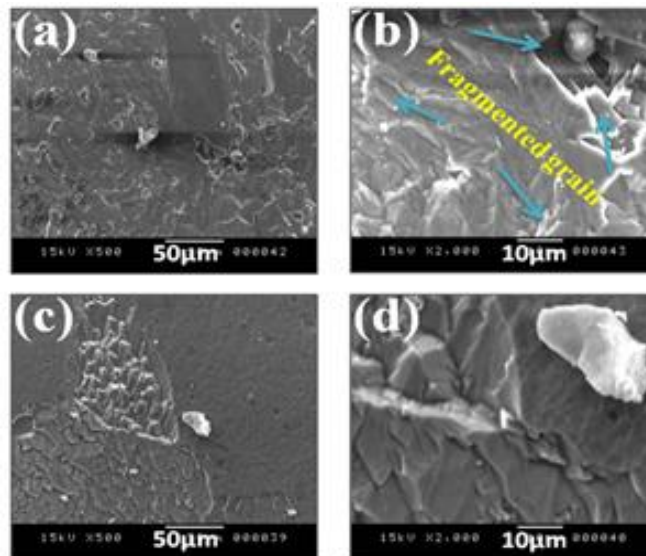


Figure. 3: SEM observation of a received state AA1050 alloy (a, b) and the homogenized AA1050 alloy at 500°C for 24 hours (c, d).

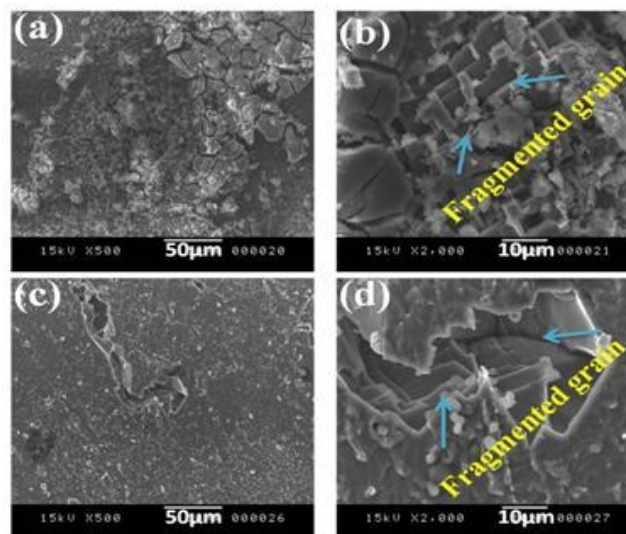


Figure. 4: SEM observation of AA1050 alloy cold-rolled with 50 % + annealing at 350°C for 1 hour (a, b) and AA1050 alloy cold-rolled with 66 % + annealing at 350°C for 1 hour (c, d).

3.2 Mechanical properties

3.2.1 Microhardness results

Data on mechanical properties (Ultimate tensile strength (U.T.S.), yield strength (Y.S.), elongation (E %) and microhardness (HV)) is summarized in table 2.

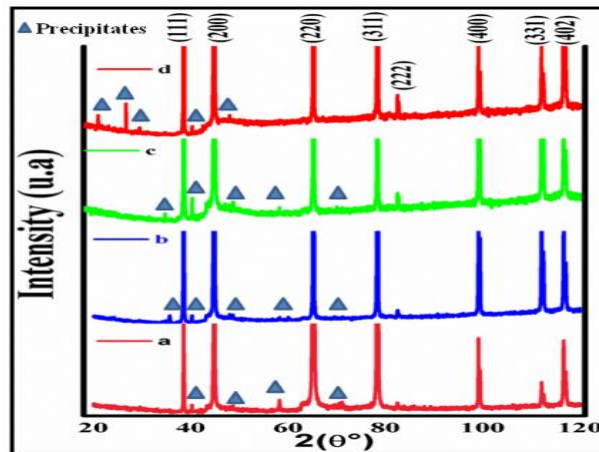


Figure. 5: The XRD patterns of a received state AA1050 alloy (a), the homogenized AA1050 alloy (b), the AA1050 alloy cold-rolled with 50 % + annealing at 350°C for 1 hour (c) and the AA1050 alloy cold-rolled with 66 % + annealing at 350°C for 1 hour (d).

Table. 2. Tensile properties and hardness of the AA1050 alloy in various conditions.

conditions	Y.S(MPa)	U.T.S(MPa)	Elongation (%)	HV (0.3)
AA1050 alloy a received state	85±1	105±1	3±2	35±2
AA1050 alloy homogenized at 500°C for 24 hours	27±1	71±1	41±2	22 ±2
AA1050 alloy cold-rolled at 50% without annealing	90±1	120±1	2.5±2	48±2
AA1050 alloy cold-rolled at 66 % without annealing	100±1	140±1	1.75±2	53±2
AA1050 alloy cold-rolled at 50% and annealed at 350°C for 1 hour	31±1	81 ±1	28±2	43±2
AA1050 alloy cold-rolled at 66% and annealed at 350°C for 1 hour	38±1	86 ±1	36±2	49 ±2

The hardness of the alloy after the homogenized treatment decreases from 35±1 HV_{0.3} to 22±1 HV_{0.3}. For as-received alloy, the microstructure is heterogeneous and there is some segregation, therefore. For the homogenized alloy, the microstructure is homogenous, some second-phase particles are dissolved or disappear, and the segregation is reduced, so the hardness is lower compared with the as-received alloy. The hardness decreases notably after homogenization. For the cold-rolled alloy, hardness increases rapidly with increasing rolling reduction. This means that there is obvious work hardening during rolling. However, the hardness changes from 43±1 HV_{0.3} to 49±1 HV_{0.3}, when the rolling reduction increases from 50 to 66 % and annealing temperature at 350°C for 1 hour, respectively. As the rolling reduction is 66 %, the hardness that is almost more two times that of the as-homogenized AA1050 alloy, indicating that the hardness can be improved by rolling. The reason is that with the increase of rolling reduction, the dislocation density increases, so the hardness increases. For annealing at 350°C for 1 hour, the hardness decreases slightly. This indicates that work hardening can be diminished effectively by annealing heat treatments, which is beneficial for the further development of wide AA1050 alloy sheets. Vickers microhardness values found in this study are with good agreement with those of X .G. Qiao et al [30] for the same material plastically deformed by ECAP material.

3.2.2 Tensile test results

For a received state AA1050 alloy, the ultimate tensile strength (U.T.S), yield strength (Y.S) and elongation are 105 ± 1 MPa, 85 ± 1 MPa and $3\pm 2\%$, respectively. Both the strength and elongation change better after homogenized treatment, (U.T.S), (Y.S) and elongation are 71 ± 1 MPa, 27 ± 1 MPa and $41\pm 1\%$, respectively. As seen, cold-rolling leads to a notable change in mechanical properties of the AA1050 alloy. With increasing cold-rolling reduction, the (U.T.S) and (YS) increase gradually, while the elongation reduces. Certainly, the improvement of the mechanical behaviour of the alloy of aluminium can be mainly attributed to the following reasons. In the first one, with increasing rolling reduction, grains are severely elongated along the rolling direction. It is advantageous for development of fiber texture along the rolling direction, which gives elevation to the improved tensile strength. Evenly with increasing rolling reduction, much more secondary phase precipitates play an important role in improving strength by precipitation strength mechanism. In the second one, with increasing rolling reduction, the work hardening is evident. This can lead to the increase of dislocations density and substructure, which results in the enhanced tensile strength and reduced elongation [22]. Although tensile strength decreases obviously and ductility increases notably after cold-rolling and annealing at 350°C for 1 hour. However, at the same time, the (U.T.S) and (Y.S) increase gradually from 81 ± 1 MPa to 86 ± 1 MPa and from 31 ± 1 MPa to 38 ± 1 MPa, when the cold-rolling reduction increases from 50 to 66 % and annealing temperature at 350°C for 1 hour, respectively. The elongation of the sample is enhanced from 28 % to 36 % respectively increasing rolling reduction and annealing. The reasons for the decreased tensile strength and the enhanced elongation are as follows. Firstly, increasing annealing temperature can give rise to increase of grain size. The grain size [d] has a significant influence on the mechanical properties of alloys, which can be explained through Hall–Petch equation [31]:

$$\sigma = \sigma_0 + \frac{k}{\sqrt{d}}$$

The smaller the grain size is, the better the mechanical properties are. The refined grains prevent the motion of dislocations from increasing the strength, and the slip systems can be changed by the blocked dislocations. Secondly, with increasing annealing temperature at 350°C for 1 hour, the secondary phase is coarser, which is bad for improving strength. Finally, the recrystallization occurs at 350°C for 1 hour and the density of dislocations decreases leading to the corresponding change of mechanical properties [32–38].

3.2.3 Fracture mechanism

Figure. 6(a-d) shows the fracture surfaces after tensile test at high magnification of AA1050 under different conditions. It shows shear zones and dimples, which are characteristics of ductile fracture. Ductile fracture normally occurs in a transgranular manner (through the grains) in metals that have good ductility and toughness. This type of fracture initiates with the nucleation, growth, and merging of microvoids near the center of the test sample [39].

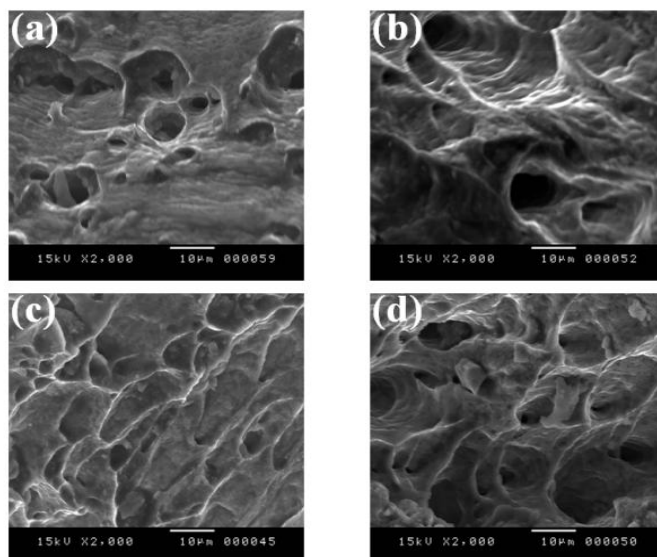


Figure. 6: Tensile fractured surfaces of AA1050 at, a received state(a), homogenized (b), cold-rolled with 50 % + annealing at 350°C for 1 hour (c) and cold-rolled with 66 % + annealing at 350°C for 1 hour(d) at high magnification

Conclusion

In view of the present data, it can be concluded that AA1050 alloy severely deformed by cold-rolling at 50% and 66%, as well as after the different metallurgical conditions, has a considerably changed properties. To study the evolution of the microstructure and associated changes of mechanical properties, the following conclusions were given below:

After homogenization at 500°C for 24 hours the material has a more uniform distribution than that of the material at a received state. Micrographs OM show the grains of AA1050 alloy have a varied shape which depends on the rate of deformation by cold-rolling. Micrographs SEM show that the structure is fragmented and the precipitates are fines, more in number and smaller in size. The XRD patterns show that AA1050 alloy has a well defined texture on the plane (220). After homogenization, the texture has been changed following the plane (200) and the same result was observed in cold-rolling with annealing at 350°C for 1 hour. Furthermore, it was noticed the presence of all the fundamental peaks on the face-centered cubic structure of the aluminum of the matrix with the existence of some secondary peaks of low intensity which could be attributed to the precipitates Al_8Fe_2Si and Al_3Fe . The tensile properties were very well improved as a function of cold-rolling and the elongation at break is also decreased. Vickers microhardness showed a good improvement from the cold-rolling.

A challenge to give balanced mechanical properties, including enhanced ductility, and reasonable strength. It's suggest that the annealing at 350°C for 1 hour after cold-rolling is the appropriate choice given that the AA1050 alloy shows a good compromise between excellent tensile proprieties, microhardness and ductility with reasonable uniform of distribution microstructure.

Acknowledgments-This work was supported by the Ministry of Higher Education and Scientific Research in Tunisia (Electromechanical Systems Laboratory (LASEM), National School of Engineers of Sfax). The authors are indebted to Dr.Aydi abdelkarim Department of Chemical and Materials Engineering, College of Engineering, Northern Border University, P.O. Box 1321, Arar, Saudi Arabia.

References

1. Loorentz Z., Young Gun Ko, *J. Alloys. Compd.* 586 (2014.) S205.
2. Kim K. J., Kim J. S., Kim C. W., Sohn I. S., Lee J. Y., Kim J. B., *Key Eng. Mater.* 353 (2007) 579.
3. Xiaoping X., Ling J., Wenjun L., Yudong L., Zhendan F., Cheng C., *Rare Metal Mat Eng.* 43 (2014) 245.
4. Meng C., Zhang D., Cui, H., Zhuang L., Zhang.,*J. Alloys Compd.* 617 (2014) 925.
5. Zhu H., Ghosh, A. K., Maruyama, K., *Mater. Sci. Eng A* .419 (2006) 115.
6. Yong Y. A. N., Zhang, Da-Tong, Cheng, Q. I. U., *Trans. Nonferrous Met. Soc. China.* 20 (2010) S619.
7. Xia S. L., Ma M., Zhang J. X., *Mater. Sci. Eng., A.* 609 (2014) 168.
8. Liu Jiantao et Morris, James G., *Mater. Sci. Eng., A.* 385 (2004) 342.
9. Ghosh M., Miroux A., et Kestens, L. A. I., *Alloys Compd.* 619 (2015) 585.
10. Cole G. S., Sherman A. M., *Mater. Charact.* 35 (1995) 3.
11. Miller W. S., Zhuang L., Bottema, *J. Mater. Sci. Eng., A.* 280 (2000) 37.
12. Starke E. A., Staley J. T., *Prog. Aerosp. Sci.* 32 (1996) 131.
13. Kang Dong-Hwan., Kim Tae-Won., *Mater. Des.* 31 (2010) S54.
14. Wyrzykowski J. W., Grabski, M. W., *Metal science.* 17(1983) 445.
15. Yu C. Y., Kao P. W., Chng C. P., *Acta Mater.*53 (2005) 4019.
16. Lloyd D., *Metal Science*, 14 (1980) 193.
17. Tsuji N., *Scripta Mater.* 47 (2002) 893.
18. Hayes, J. S., Keyte R., Prangnell P. B., *Mater. Sci. Technol.* 16 (2000) 1259.
19. Mishin O. V., *Acta Mater.*61 (2013)5354.
20. Liu D. H., Yu H. P., Li C. F., *Mater. Sci. Eng., A.* 551 (2012) 280.
21. Min Z. H. A., *Trans. Nonferrous Met. Soc. China.*24 (2014) 2301.
22. Bo W. A. N. G., Chen X. H., Pan F. S., Mao J. J., Yong F. A. N. G., *Trans. Nonferrous Met. Soc. China* 25 (2015) 2481.
23. El-Danaf Ehab A., *Mater. Sci. Eng., A.* 487 (2008) 189.
24. El-Danaf Ehab A., *Mater. Des.* 34 (2012) 793.
25. El-Danaf Ehab A., *Mater. Des.* 32 (2011) 3838.

26. Han J. H., Seok, H. K., Chung, Y. H., Shin, M. C., Lee, J. C., *Mater. Sci. Eng., A*. 323 (2002) 342.
27. Koroleva E. V., Thompson, G. E., Skeldon, P., Hollrigl, G., Smith, G., Lockwood, S., *Electrochim. Acta*. 50(2005) 2091.
28. Buytaert G., Terryn H., Van Gils S., Kernig B., Grzembera B., Mertens M., *Surf. Interface Anal.* 38 (2006) 272
29. Garcia-Garcia F. J., Skeldon P., Thompson G. E., Smith G. C., *Electrochim. Acta*, 75 (2012) 229.
30. Qiao X. G., Starink M. J., Gao N., *Mater. Sci. Eng., A*. 513 (2009) 52.
31. William D C, David G R., *Materials science and engineering: an introduction*. 8th ed, Versailles (2009).
32. Lu S. L., Wu S. S., Zhu Z. M., Ping A. N., Mao Y. W., *Trans. Nonferrous Met. Soc. China*. 20 (2010) s758.
33. Roy Shibayan, *Mater. Sci. Eng., A* .528 (2011) 8469.
34. Song H. R., Y. S. Kim W., Nam J., *Met. Mater. Int.* 12 (2006) 7.
35. Liu Jian-guang X., Wei U. E., *Trans. Nonferrous Met. Soc. China*. 23 (2013) 964.
36. Jong-Jin P., *J. Mater. Process. Technol.*.87 (1999) 146.
37. Jobba M., Mishra R. K., Niewczas M., *Int. J. Plast.* 65 (2015) 43.
38. Wen Wei, J. G. Morris., *Mater. Sci. Eng., A* .373 (2004) 204.
39. Gashti S. O., *J. Alloys Compd.* 688 (2016) 44

(2017); <http://www.jmaterenvironsci.com>